Interaction of Two Parallel Cracks in REBCO Bulk Superconductors under Applied Magnetic Field *

Zhao-Xia Zhang(张朝霞)[1], Feng Xue(薛峰)[2], Xiao-Fan Gou(苟晓凡)[2**]

[1]*Faculty of Civil Engineering & Mechanics, Jiangsu University, Zhenjiang 212013*
[2]*College of Mechanics and Materials, Hohai University, Nanjing 210098*

(Received 9 December 2015)

Interactions of two collinear and parallel a/b-plane cracks in REBCO (where RE is a rare-earth element and usually Y is adopted) bulk superconductors under the Lorentz force resulted from the applied magnetic field are studied. By using the derived boundary integral equation for the crack problem of a cylindrical bulk superconductor under the applied magnetic field, we comprehensively investigate the stress intensity factor (SIF) of modes I and II at the crack tips of the two collinear and parallel cracks with their sizes, relative positions and the applied magnetic field. The calculated results show that in most cases, the SIF of mode I is found to be about tens of times of the one of mode II, and all the SIFs are always proportional to increase in the applied magnetic field, and the cracks near the center are more dangerous due to the larger Lorentz force.

PACS: 74.72.−h, 74.25.Ld, 62.20.mt DOI: 10.1088/0256-307X/33/7/077401

Melt-grown REBCO (where RE is a rare-earth element, and usually Y is adopted) single grain bulk is highly attractive for many practical applications.[1,2] In particular, the REBCO bulk can be used for permanent magnets because it can trap very high magnetic field of several tesla or even higher at low temperatures.[1] For a magnet of larger volume REBCO single grain bulk superconductor, in addition to the effort of improving the critical current density,[3] in-depth understanding of the crack strength under the Lorentz force resulting from the applied magnetic field is really important.[1]

For such an REBCO bulk superconductor with a large number of cracks, in addition to cracking in the process of cooling down during the initial fabrication, when it is magnetized by the applied magnetic field at low temperature ($< T_c$), the crack growth under the Lorentz force resulting from the induced current in the bulk superconductor has been the other serious problem.[4−6] So far researchers have made great efforts,[5,7,8] in which the theoretical studies based on the related works of some fabrication techniques (for example, Ag addition[5]) and experimental observations has been an important aspect. Noticeably, Zhou *et al.* have made persistent efforts on the crack problem of superconductors, and obtained some significant results.[9−11] In particular, for a central crack and two collinear cracks[11] in a slab superconductor, and a central crack[9,10] in a long cylindrical superconductor, the singular stress field and the stress intensity factors at the crack tips were accurately calculated.

For a cylindrical bulk superconductor under the applied magnetic field, the a/b-plane ((001) plane) is the first cleavage plane since the fracture toughness $K_{IC} = 0.32\,\mathrm{MPa{\cdot}m^{1/2}}$ is the lowest there.[5] In this Letter, we concentrate on two collinear and parallel cracks in the a/b-plane of an REBCO cylindrical bulk superconductor, and theoretically evaluate the crack strength and interaction between each other under Lorentz force resulting from the applied magnetic field on the base of our previous work of the derived boundary integral equation (BIE).[12]

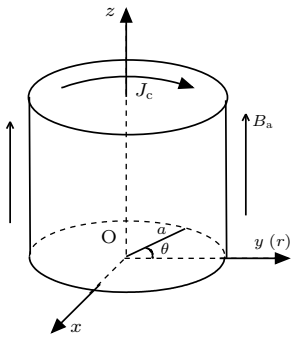

Fig. 1. A cylindrical bulk superconductor in the applied magnetic field. Here B_a is the applied magnetic field, and J_c is the critical current density.

Here we consider a cylindrical bulk superconductor, which is the typical shape of melt-grown REBCO single grain bulks.[1,13] When it is in an applied uniform magnetic field, as shown in Fig. 1, according to the Maxwell equations, and in the assumption of the Bean critical model (the critical current density J_c keeps a constant),[14] the distribution of magnetic field

*Supported by the National Natural Science Foundation of China under Grant Nos 11372096 and 11402073, the National Research Foundation for the Doctoral Program of Higher Education of China, and the Natural Science Foundation of Jiangsu Province under Grant No BK20130824.

**Corresponding author. Email: xfgou@hhu.edu.cn

© 2016 Chinese Physical Society and IOP Publishing Ltd

from the induced current can be given as

$$B(r) = \mu_0 J_c r + C, \quad (0 < r \le a), \tag{1}$$

where $\mu_0 = 4\pi\times10^{-7}\,\mathrm{N/A^2}$ is the permeability of vacuum, and a is the radius of the cylinder bulk superconductor. The constant C can be determined by the magnetic field B at the boundary of the cylinder bulk (i.e., from $r = a$, $B = B_a$, and $C = B_a - \mu_0 J_c a$, where B_a is the magnetic field intensity at the boundary). In particular, when the applied magnetic field just fully penetrates the bulk, we denote $B_a = B_p$, where $B_p = \mu_0 J_c a$.

Thus the Lorentz force of the induced current under the applied magnetic field can be obtained by

$$F_L(r) = \mu_0 J_c^2 (r - a) + J_c B_a. \tag{2}$$

Under the above body Lorentz force, for an elastic cylinder, its mechanical response is actually an axisymmetric problem. According to the elastic theory,[15] in the system of polar coordinates (r, θ, z) (shown in Fig. 1), the equilibrium equation with the radial displacement u_r as the unknown variable can be written as

$$\frac{d^2u_r}{dr^2} + \frac{1}{r}\frac{du_r}{dr} - \frac{u_r}{r^2} = -F_L\frac{(1+\nu)(1-2\nu)}{E(1-\nu)}, \tag{3}$$

where E is Young's modulus, and ν is the Poisson ratio of the bulk superconductor. Then, the radial and hoop stresses can be analytically obtained as

$$\sigma_r = f\frac{3-2v}{8(1-\nu)}(a^2 - r^2) + k\frac{2-v}{3(1-\nu)}(a - r), \tag{4}$$

and

$$\sigma_\theta = \frac{1}{8}f\Big[(3a^2 - r^2) + \frac{v}{1-v}(a^2 - 3r^2)\Big] + \frac{1}{3}k\Big[(2a - r) + \frac{v}{1-v}(a - 2r)\Big], \tag{5}$$

where

$$k = J_c B_a - \mu_0 J_c^2 a, \quad f = \mu_0 J_c^2. \tag{6}$$

According to Eqs. (4) and (5), the stress reaches the maximum when $r = 0$, and it can be given as

$$\sigma_r = \sigma_\theta = \frac{1}{(1-\nu)}\Big(\frac{3-2\nu}{8}fa^2 + \frac{2-\nu}{3}ka\Big). \tag{7}$$

Thus substituting Eq. (6) into Eq. (7), and considering the penetrated field induction B_p, we can further obtain

$$\sigma_r = \sigma_\theta = \frac{(9-6v)B_p^2 + (16-8v)B_p(B_a - B_p)}{24(1-v)\mu_0}. \tag{8}$$

When the cylinder bulk is just fully penetrated, $B_a = B_p$. In this case, the characteristic stress σ_0 ($=\sigma_r = \sigma_\theta$) is introduced, and from Eq. (8), it can be simplified to

$$\sigma_0 = \frac{(9-6v)}{24(1-v)}\frac{B_p^2}{\mu_0}. \tag{9}$$

Based on the boundary integral equation presented by Wang *et al.*,[16] Chau *et al.*,[17] and later developed by Zhang *et al.*,[12,18] for a multiply connected domain Ω containing holes and cracks whose boundaries are denoted by S and Γ, respectively, we derive the BIE taking account of the Lorentz force induced from the applied magnetic field.

To solve a crack problem, we can introduce a complex unknown function $H(t)$ as

$$H(t) = \frac{i}{\kappa+1}[p(t) - iw(t)]e^{-i\alpha(t)}, \tag{10}$$

where

$$p(t) = \begin{cases} t_1(t) + it_2(t), & t \in S, \\ \sum t_1(t) + i\sum t_2(t), & t \in \Gamma, \end{cases} \tag{11}$$

and

$$w(t) = \begin{cases} 2G\frac{\partial}{\partial s(t)}[u_1(t) + iu_2(t)], & t \in S, \\ 2G\frac{\partial}{\partial s(t)}[\Delta u_1(t) + i\Delta u_2(t)], & t \in \Gamma, \end{cases} \tag{12}$$

where κ equals $3-4\nu$ for plane strain and $(3-\nu)/(1+\nu)$ for plane stress, G is the shear modulus of the body, the traction and displacement data on the field points t are denoted as $t_j(t) = \sigma_{ij}n_i$ and $u_j(t)$, respectively, $(i, j = 1, 2)$. Finally, we can obtain the BIE with the complex unknown function $H(t)$ as follows:

$$\pi i f(t_0) = \int_{S+\Gamma}\Big\{\frac{H(t)}{t - t_0} - \frac{\overline{H(t)}}{\bar{t} - \bar{t}_0}e^{-2i\alpha(t)} + e^{-2i\alpha(t_0)}\Big[\frac{H(t) - q(t)}{\bar{t} - \bar{t}_0} + \frac{t - t_0}{(\bar{t} - \bar{t}_0)^2}\overline{H(t)}e^{-2i\alpha(t)}\Big]\Big\}dt, \tag{13}$$

where

$$f(t_0) = \begin{cases} \sigma_n(x_0) + i\sigma_{ns}(x_0), & t \in S, \\ \sigma_n(x_0^+) + \sigma_n(x_0^-) + i[\sigma_{ns}(x_0^+) + \sigma_{ns}(x_0^-)], & t \in \Gamma. \end{cases} \tag{14}$$

In Eq. (13), $q(t) = ip(t)e^{-ix(t)}$ is the surface force acting on the crack boundary, and $t_0 = x_{01} + ix_{02}$ is the point on the boundary $S + \Gamma$; $+$ and $-$ represent the upper and lower crack surfaces, respectively. For a cylindrical superconductor in applied uniform magnetic field as shown in Fig. 1, under the Lorentz force,

if the stress has been obtained by Eqs. (4) and (5), when $t \in \Gamma$, Eq. (14) can be rewritten as

$$\begin{aligned} f(t_0) =& [\sigma_\theta^+(t_0) + \sigma_\theta^-(t_0)]_n + i[\sigma_{\rm r}^+(t_0) \\ &+ \sigma_{\rm r}^-(t_0)]_{ns} + [\sigma_{\rm r}^+(t_0) + \sigma_{\rm r}^-(t_0)]_n \\ &+ i[\sigma_\theta^+(t_0) + \sigma_\theta^-(t_0)]_{ns}, \text{ if } t_0 \in \Gamma, \quad (15) \\ q(t) =& [\sigma_\theta^+(t) - \sigma_\theta^-(t)]_n + i[\sigma_{\rm r}^+(t) - \sigma_{\rm r}^-(t)]_{ns} \\ &+ [\sigma_{\rm r}^+(t) - \sigma_{\rm r}^-(t)]_n + i[\sigma_\theta^+(t) \\ &- \sigma_\theta^-(t)]_{ns}, \text{ if } t \in \Gamma. \quad (16) \end{aligned}$$

For solving the BIE (13), the single displacement condition is given as[17,18]

$$\begin{aligned} \int_\Gamma H(t)ds(t) =& \{(p_\theta^+ + p_\theta^-)_n + (p_{\rm r}^+ + p_{\rm r}^-)_n \\ &+ i[(p_\theta^+ + p_\theta^-)_{ns} \\ &+ (p_{\rm r}^+ + p_{\rm r}^-)_{ns}]\}/[(\kappa+1)]. \quad (17) \end{aligned}$$

In the following, for the two typical a/b-plane cracks of collinear and parallel cracks, based on the above derived BIE, we will calculate the stress intensity factor (SIF) at the crack tips, and its variation with their relative positions and sizes.

(i) Case I: the same two collinear cracks (red lines) with a horizontal separation are symmetrically located at the center of the cylindrical superconductor. As shown in Fig. 2(a), the relative horizontal position between each other can be specified as the ratio d/c, where $2d$ and $2c$ are the distance between their closer tips and the length of the cracks, respectively.

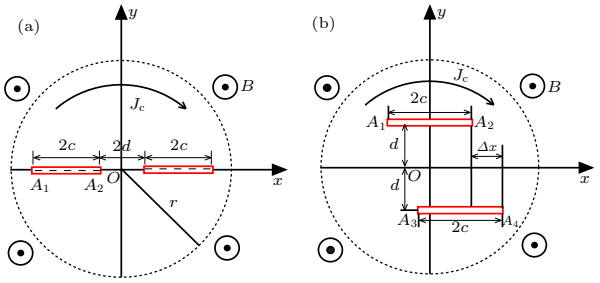

Fig. 2. (a) Two collinear cracks symmetrically located at the center of the cylindrical superconductor in the applied magnetic field. (b) Two parallel cracks with a horizontal separation located at the center of the cylindrical superconductor in the applied magnetic field. The crack A_1A_2 is assumed to be fixed symmetrically with the y-axis, and the other could have a horizontal translation of the distance Δx.

We calculate the SIF at the crack tips A_1 and A_2 (see Fig. 2(a)), and plot the normalized one with the parameter d/c and the applied magnetic field in Figs. 5 and 6, respectively. It can be found that the normalized SIFs at the tip A_1 and A_2 decrease with d/c, and the value at the tip A_2 is much larger than that at the tip A_1, especially in the range $d/c < 1.0$ (as shown in Fig. 2(a), and the tip A_2 is near while the tip A_1 is far away from the center). For the SIF at the tip A_2, we can also find that the SIF sharply reduces when $d/c < 1.0$, and slowly varies when $d/c > 1.4$. The SIF at the tip A_2 can reach 1.5 when $d/c = 0.1$, and both are gradually close to 1 when $d/c > 1.6$. This result clearly indicates that the SIF is very sensitive to the position of the crack, especially for the tip A_2 when the crack is close to the center of the cylindrical bulk superconductor. Thus for such collinear cracks near the center of the bulk superconductor, under the Lorenz force resulting from the induced current in the applied magnetic field, the crack is very possibly grown at the tips near the center.

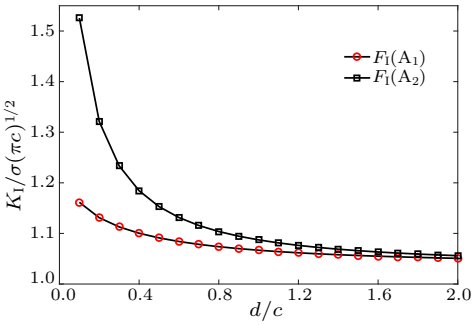

Fig. 3. Normalized stress intensity factors (SIFs) of mode I (defined as $K_{\rm I}/\sigma\sqrt{\pi c}$) at the crack tips ($A_1$ and A_2) versus d/c.

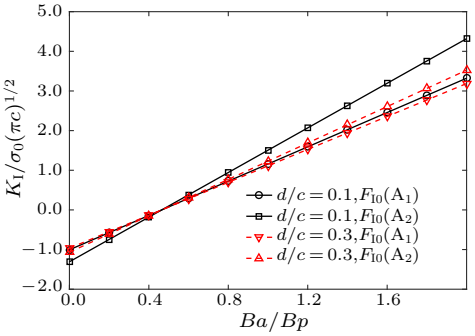

Fig. 4. Normalized SIFs of mode I (defined as $K_{\rm I}/\sigma_0\sqrt{\pi c}$, where σ_0 is related to the magnetic field $B_{\rm p}$) at the crack tips (A_1 and A_2) versus the applied magnetic field $B_{\rm a}/B_{\rm p}$ in the two cases of d/c (=0.1 and 0.3).

For exploring the effect of the applied magnetic field on the SIF at the crack tips, σ_0, instead of σ in Fig. 3, is introduced. If $\nu = 0.25$,[19] the characteristic stress σ_0 from Eq. (9) can be simplified to $\sigma_0 = B_{\rm p}^2/2.4\mu_0$. Then, the normalized SIF at the crack tips with the applied magnetic field $B_{\rm a}/B_{\rm p}$ in the two cases of d/c is calculated as shown in Fig. 4. Obviously, the SIF is always proportional to increase in $B_{\rm a}/B_{\rm p}$. For the same case of d/c, the SIF at the crack tip A_2 is always larger than that at the tip A_1, and the variations of the SIF at the tips A_1 and A_2 have an intersection point (where $K_{\rm I}/\sigma_0\sqrt{\pi c} = 0$). In the case of the smaller d/c (=0.1), the SIF at the same tip is larger, and also the difference between the SIFs at the tips A_1 and A_2 is larger. In other words,

the slopes of linear increase of the normalized SIF via B_a/B_p are close to each other for the cracks that are far away from the center (corresponding to the case $d/c = 0.3$), while they are apart from each other for the cracks that are near the center (corresponding to the case $d/c = 0.1$). Thus for collinear cracks near the center of the bulk, the larger the applied magnetic field is, the greater the SIF is, and the crack will first grow at the tip that is closer to the center under the Lorentz force.

(ii) Case Ⅱ: two parallel cracks are also located at the center of the cylindrical superconductor. As shown in Fig. 2(b), in addition to the parameter d/c, the other is introduced to specify the relative horizontal separation, where Δx denotes the horizontal separation.

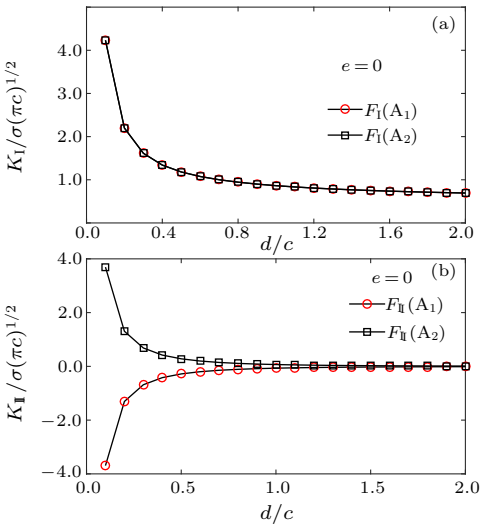

Fig. 5. The normalized SIFs of modes (a) I and (b) Ⅱ (in which the SIF of mode Ⅱ is defined as $K_{\rm II}/\sigma\sqrt{\pi c}$) at the crack tips ($A_1$ and A_2) versus d/c in the case of $e(=\Delta x/c) = 0$.

For this case, we investigate the SIF of both models I and Ⅱ of the crack tips and the dependences on the relative position parameters (d/c and e) and the applied magnetic field. In the special case of $e = 0$ (i.e., without horizontal separation), we calculate the normalized SIF of both models I and Ⅱ at the crack tips A_1 and A_2 of the crack A_1A_2 with d/c, as shown in Fig. 5. For mode-I SIF (Fig. 5(a)), obviously the SIFs at the tips A_1 and A_2 are almost the same for the symmetrical arrangement of parallel cracks. The SIFs are larger when d/c is smaller ($d/c < 0.6$), and then sharply decrease with d/c ($d/c > 1.0$). For mode-Ⅱ SIF (Fig. 5(b)), obviously the variation of the SIFs at the crack tips A_1 and A_2 with d/c are exactly opposite to each other, which results from the opposite directions of the Lorentz force on the two tips in the case of $e = 0$. In this case we find that modes I and Ⅱ SIFs are of almost the same order of magnitude, and also their variations with d/c are similar. Thus for this case ($e = 0$) we can conclude that the cracks closer to each other and near the center will most possibly grow under the Lorentz force.

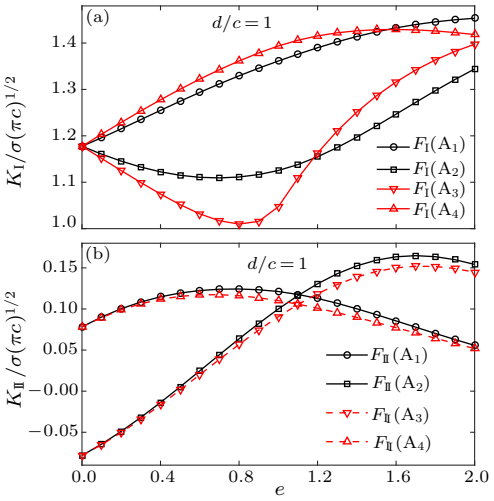

Fig. 6. The normalized SIFs of modes (a) I and (b) Ⅱ at the crack tips (A_1, A_2, A_3 and A_4) versus e ($=\Delta x/c$) in the case of $d/c = 1$.

To investigate the strength of the parallel cracks with a horizontal separation under the Lorentz force, we further calculate the normalized SIFs of both models I and Ⅱ at the crack tips A_1 and A_2 of the crack A_1A_2 and at the crack tips A_3 and A_4 of the crack A_3A_4 with e (d/c is fixed at 1), as shown in Fig. 6. For mode-I SIF (see Fig. 6(a)), we can find that the variation of SIF at the tip A_1 is similar to that at the tip A_4: the SIFs keep slowly increasing or first increasing and then decreasing with e; due to the fact that the interaction between the cracks, the variations of SIF at the tips A_2 and A_3 are different from those at the tips A_1 and A_4: with increasing e, the SIFs first decrease and then increase as the inflection point $e = 0.8$, and the variation of the SIF at the tip A_3 is more dramatic. For mode-Ⅱ SIF (Fig. 6(b)), the similar variations of the SIF are for the tips A_1 and A_4, and also for the tips A_2 and A_3, while the variations of the two groups are quite different. The range of the variation of the SIFs at the tips A_2 and A_3 is much larger; the SIFs always first increase and then decrease, while the inflection points are different for the two groups: for the tips A_1 and A_4, the point is about $e = 0.8$, while for the tips A_2 and A_3 it is about $e = 1.6$. From Fig. 6, as a whole, (1) the value of mode-I SIF is much larger than that of mode-Ⅱ SIF, which means that mode I is primary, and dominates the fracture failure in this situation; (2) for mode I, the values of the SIF at the tips A_1 and A_4 are larger, and the variations at the tips A_2 and A_3 are more complicated.

Figure 7 shows the variation of the normalized SIF $K_{\rm I}/\sigma_0\sqrt{\pi c}$ (where σ_0 is the same as that in case I) of modes I and Ⅱ with the applied magnetic field in the case of $e = 1$ and $d/c = 1$. For both the modes I and

Ⅱ SIFs, on the whole, we can find: (1) the SIFs are always proportional to increase with B_a/B_p; (2) similar to Fig. 6, the value of the SIFs shows that mode-I SIF plays as the dominator; (3) similar to the result in Fig. 4, the variations of the SIFs at the different tips always have an intersection point (where $K_I/\sigma_0\sqrt{\pi c}=0$ and $K_{II}/\sigma_0\sqrt{\pi c}=0$). Thus for the case of two parallel cracks ($e=1$, $d/c=1$), with increasing the applied magnetic field, correspondingly the Lorentz force linearly increases, and the cracks tend to grow. Mode-I SIF is always primary, and dominates the fracture strength at the crack tips. For both modes I and Ⅱ SIFs, the crack growth initiates at the crack tips A_1 and A_4.

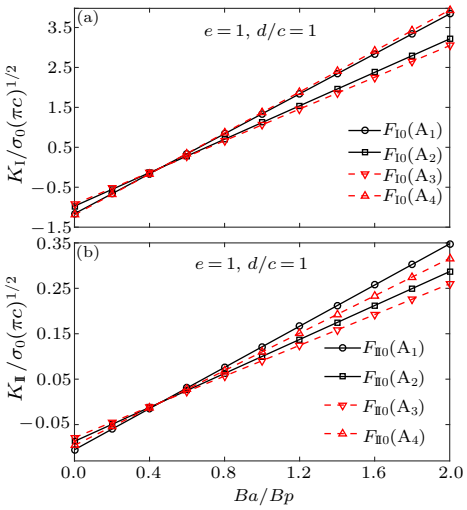

Fig. 7. The normalized SIFs of modes (a) I and (b) Ⅱ (defined as $K_{II}/\sigma_0\sqrt{\pi c}$, where σ_0 is the same as that in case I) at the crack tips (A_1, A_2, A_3 and A_4) versus the applied magnetic field B_a/B_p in the case of $e=1$ and $d/c=1$.

In fact, the crack problem in bulk superconductors is more complicated. In a large volume bulk superconductor, actually cracks exist with the length of multiple different scales ranging from several microns to dozens of microns, even to millimeter level coexisting.[5] In contrast, for the larger cracks with the length of several millimeters (i.e., macro cracks), here we must take into account of the effect of cracks on the distribution of the induced superconducting current, and further the magnetic field in superconductors. Therefore, more in-depth studies on the crack problem under the magnetic field in bulk superconductors need to be continued.

In conclusion, for an REBCO cylindrical bulk superconductor in the applied magnetic field, using the derived boundary integral approach, we have studied the fracture strength of the two collinear and parallel cracks in the a/b-plane under the Lorentz force resulting from the applied magnetic field. The calculated results show that the cracks (collinear and parallel cracks) near the center of the bulk are more dangerous, and also both modes I and Ⅱ SIFs are always proportional to increase in the applied magnetic field B_a/B_p. For the collinear cracks, the crack growth initiates at the crack tip that is closer to the center of the bulk superconductor. Especially for parallel cracks without horizontal separation (i.e., $e=0$), modes I and Ⅱ SIFs are equally important, while mostly for the cracks with horizontal separation (i.e., $e\neq 0$), mode I is primary, and dominates the fracture strength of cracks. For the latter case, with increasing e in the range of $0\leq e\leq 2$ the SIF of modes I first increases and then slightly decreases for the crack tips away from each other, while first decreases and then increases for the tips close to each other.

References

[1] Tomita M and Murakami M 2003 *Nature* **421** 517
[2] Zhang Z Y, Matsumoto S, Teranishi R and Kiyoshi T 2012 *Supercond. Sci. Technol.* **25** 115012
[3] Salama K, Selvamanickam V, Gao L and Sun K 1989 *Appl. Phys. Lett.* **54** 2352
[4] Gruss S, Fuchs G, Krabbes G, Verges P, Stöver G, Müller K H, Fink J and Schultz L 2001 *Appl. Phys. Lett.* **79** 3131
[5] Diko P 2004 *Supercond. Sci. Technol.* **17** R45
[6] Tom H J 2000 *Supercond. Sci. Technol.* **13** R121
[7] Gou X F, Zheng X J and Zhou Y H 2007 *IEEE Trans. Appl. Supercond.* **17** 3795
[8] Diko P 1998 *Supercond. Sci. Technol.* **11** 68
[9] Yong H D, Zhou Y H and Zeng J 2008 *J. Appl. Phys.* **104** 113902
[10] Zeng J, Zhou Y H and Yong H D 2010 *J. Appl. Phys.* **108** 033901
[11] Gao Z W, Zhou Y H and Lee K Y 2010 *Physica* C **470** 654
[12] Zhang Z X, Chen W and Gou X F 2015 *AIP Conf. Proc.* **1648** 490012
[13] Krabbes G, Fuchs G, Canders W R, May H and Palka R 2006 *High Temperature Superconductor Bulk Materials: Fundamentals, Processing* (New Jersey: John Wiley & Sons Inc.)
[14] Bean C P 1962 *Phys. Rev. Lett.* **8** 250
[15] Xu Z 2006 *Elasticity* (Beijing: Higher education press)
[16] Wang Y B and Chau K T 1997 *Int. J. Fract.* **87** 1
[17] Chau K T and Wang Y B 1999 *Int. J. Solids Struct.* **36** 2041
[18] Zhang Z X, Wang Y B and Yang S H 2004 *J. Lanzhou University* **40** 16 (in Chinese)
[19] Qiu X G 2011 *High-Temperature Superconductors* (Cambridge: Woodhead Publishing) p 164